J. Math. Biol. (1998) 37: 203–234

Journal of Mathematical Biology

Gain-induced oscillations in blood pressure

Roselyn M. Abbiw-Jackson[1], William F. Langford[2,3,⋆]

[1] Department of Mathematics, University of Maryland, College Park, MD 20742, USA
[2] Department of Mathematics and Statistics, University of Guelph, Guelph ON, Canada N1G 2W1
[3] The Fields Institute for Research in Mathematical Sciences, 222 College Street, Toronto ON, Canada M5T 3J1

Received: 15 September 1997/Revised version: 15 March 1998

Abstract. "Mayer waves" are long-period (6 to 12 seconds) oscillations in arterial blood pressure, which have been observed and studied for more than 100 years in the cardiovascular system of humans and other mammals. A mathematical model of the human cardiovascular system is presented, incorporating parameters relevant to the onset of Mayer waves. The model is analyzed using methods of Liapunov stability and Hopf bifurcation theory. The analysis shows that increase in the gain of the baroreflex feedback loop controlling venous volume may lead to the onset of oscillations, while changes in the other parameters considered do not affect stability of the equilibrium state. The results agree with clinical observations of Mayer waves in human subjects, both in the period of the oscillations and in the observed age-dependence of Mayer waves. This leads to a proposed explanation of their occurrence, namely that Mayer waves are a gain-induced oscillation.

Key words: Mayer waves – Hopf bifurcation – Cardiovascular instability – Baroreflex control – Gain-induced oscillations

1 Introduction

The existence of fluctuations in blood pressure has been know since the introduction of the recording manometer by C. Ludwig (see [20]). These fluctuations, usually referred to as waves, are classified by various methods including the name of the discoverer, the origin, physiological cause, or the frequency or period. The term Mayer waves

⋆ Research supported by NSERC (Canada). Correspondence to: wlangfor@uoguelph.ca

refers to periodic fluctuations in blood pressure which are slower than respiration in animals with normal respiratory movements, and appear to be independent of normal heartbeat and respiration. They were reported by S. Mayer in 1876 [17], and hence the name. They are also known as third order waves or ten second waves.

The frequencies reported by various authors for Mayer waves differ considerably [20]. Those described by Mayer in rabbits had a frequency of 6–9 min^{-1}, while other researchers have found waves with frequencies ranging from 7–12 min^{-1} in humans [20]. These frequencies correspond to periods of 5–10 seconds. Hence, some researchers have proposed to designate these waves as the "10-second-rhythm" [20]. The onset of Mayer waves may result in serious physiological implications, such as fainting. Mayer waves are of interest to researchers seeking to understand fully the functioning of the cardiovascular system.

It is generally conceded that Mayer waves appear most often when the subjects are exposed to abnormal conditions [2]. Lack of oxygen, the effects of severe haemorrhage, and other extreme or sudden changes in blood supply to parts of the body favour the appearance of these slow periodic fluctuations [2]. Experiments have shown that when the blood pressure is measured for subjects lying in a supine position and then in a tilted position, there may exist Mayer-like oscillations for the tilted position. A remarkable feature observed in these experiments is that the Mayer waves occur more frequently in younger subjects, and disappear with age [6, 12, 14, 16, 18, 19]. The origin of Mayer waves, however, remains an unsolved problem [20]. At a conference on Mayer waves held in Prague in 1977, various theories were proposed to explain the origin of these waves. Four main theories, the myogenic theory, the central theory, the feedback theory, and the resonance theory were given.

The myogenic theory states that Mayer waves are due to the inherent property of peripheral systems, (vascular smooth muscle), to exhibit spontaneous rhythmic activity. The central theory postulates that cardiovascular centres in the brain stem generate the slow rhythms in a way similar to the respiratory centre. The feedback theory, as its name suggests, attributes the origin of Mayer waves to delays and nonlinearities in the body's feedback control mechanisms. The resonance theory postulates that one or more of the above factors enable the overall circulatory system to resonate at certain frequencies, but this has never been substantiated. Among the four, the feedback theory and the central theory have been considered most probable by several authors [13, 23, 24]. However, the stability of the central oscillator is questionable [23]. Thus, among the favored theories, the

feedback theory remains the most probable explanation for the existence of Mayer waves.

It is essential, for survival, that blood pressure be controlled to stay within a narrow, safe range. This function is performed by the body's feedback control mechanisms, the fastest being the baroreflex. The baroreceptors are nonlinear stretch sensors located in the systemic arteries which detect changes in blood pressure. The baroreflex feedback loops respond to baroreceptor impulses to control blood pressure via three mechanisms: changes in heart rate, systemic capillary resistance and venous volume. All three mechanisms are explored in this work.

DeBoer et al. [5] proposed that Mayer waves are caused by a time delay in the baroreceptor feedback loop. If this were the case, one would expect the delay to increase with age due to a slowing of the body's responses. This would then cause an increase in the existence of Mayer waves in older people, in contradiction to the experimental evidence. It is well known that time-delays can induce oscillations in control systems [9]; however, the actual time delays in the baroreflex control loop are orders of magnitude smaller than the observed period. While we do not discount the existence of a feedback delay, it does not appear to be the main cause of Mayer waves. We hypothesize instead that blood pressure oscillations may be attributed to a change in feedback gain, extending the work of Wesseling et al. [23, 24]. Previous studies of feedback-control systems in physiology (Glass and Mackey model) [7, 15], and in engineering (Watt's regulator model) [10, 21], have shown that an increase in feedback gain can cause a system to change behaviour from a steady state to an oscillating state. This phenomenon may be called a "gain-induced oscillation" and it can be studied by use of the Hopf bifurcation theorem. Since young adult humans tend to have quicker reflexes and better muscle tone than the elderly, they can be expected to have higher gain in the baroreceptor loop. Thus our hypothesis that Mayer waves may be a gain-induced instability is consistent with the observed age-related data.

A mathematical model can be used to give greater insights into the roles of the various mechanisms affecting Mayer waves. Thus the primary objective of this study is to develop a dynamical model for the mammalian circulatory system and use it to explore blood pressure dynamics, as a function of the physiological parameters in the model. The new dynamical model presented here is a generalization of the steady-state model of Hoppensteadt and Peskin [11]. In addition to incorporating temporal dynamics, this model will allow investigation of the effects of each of the three baroreflex feedback loops, independently of the other two. This type of experiment has been performed by

severing nerves in animals, e.g. dogs [22], but is difficult to carry out on live human subjects. Parameter values in the mathematical model are chosen to correspond to a typical adult human being. The results of the analysis show that an increase in the nonlinear gain in the baroreceptor feedback loop (even without introducing time delays) is sufficient to produce oscillations which closely resemble the observed Mayer waves in humans.

2 Modeling

While it is desirable to include the behaviour of each cardiovascular component in a model of the circulation, certain components can be lumped together without sacrificing the qualitative behaviour of the system [3, 16]. This section presents the modeling assumptions and the development of the model, first for the basic fluid flow of blood in the cardiovascular system, then with the addition of nonlinear baroreflex control.

2.1 Modeling assumptions

The assumptions and simplifications underlying the mathematical model are stated in the following.

1. The cardiovascular system is a closed-looped hydrodynamic system comprised of two heart pumps (the left and right sides of the heart), two large arteries, two veins and two capillary networks, corresponding to the systemic and pulmonary circulations respectively. The total blood volume is constant in time.
2. The large arteries and veins and the heart are compliance vessels, that is, volume is proportional to pressure in these vessels [11]. On the other hand, the smaller arteries and veins in the capillary networks are resistance vessels, that is, flow is proportional to pressure [11]. The unstressed volume of the blood vessels is negligible in all parts of the circulation except for the systemic veins.
3. Flow from the heart is continuous, that is the pulsatile nature of blood pressure is neglected and only average pressures and volumes, over the period of the pulse, are dealt with.
4. The pressure in the heart when relaxed, is equal to that of the veins supplying blood to it. That is, the pressure in the right and left hearts are those of the systemic and pulmonary veins respectively. On its

expansion stroke (diastole) the heart receives a volume of blood proportional to this venous pressure. The heart pumps out at each contraction stroke (systole) the amount of blood received from the veins on the previous diastole. This is the Frank-Starling model of the heart [24].

5. Cardiovascular blood pressure is controlled by a baroreceptor feedback mechanism, which acts to change systemic venous unstressed volume, systemic venous compliance, systemic capillary resistance and the heart rate, in order to counteract changes in systemic arterial pressure.
6. The baroreceptor feedback gain and its dependence on systemic arterial pressure is modeled as being a Hill function (defined below).
7. Changes in venous volume, systemic resistance and heart rate act independently and in parallel, on blood pressure.
8. Compliance is constant in each part of the cardiovascular system except the systemic veins, where it may be varied by the baroreflex.
9. Resistance is constant for the capillary networks of the pulmonary circulation, but may be varied by the baroreflex in the systemic circulation.

2.2 Model development

A notational convention adopted throughout this model is that dynamic variables are represented by lower case letters, while parameters and labels are written in upper case. We first construct a simple linear model of the cardiovascular system, and then add the baroreflex control system.

2.2.1 Linear cardiovascular model

The following linear relationship between volume v, pressure p, and compliance C, in the large vessels (arteries and veins) of the circulation [11], is the mathematical form of Assumption 2. (i.e. that these are compliance vessels)

$$v = C \cdot p \tag{1}$$

There are four such equations in the model, corresponding to the systemic arteries and veins, and the pulmonary arteries and veins, for which the variables v, p, C are distinguished by subscripts SA, SV, PA, PV respectively. However, Eq. (1) suggests that if $p = 0$, then $v = 0$, which is not the case, especially in the systemic veins which typically contain about 70% of the blood in a human body. A more realistic

relation to be used for the case of the systemic veins is:

$$v_{SV} = C_{SV} \cdot p_{SV} + V_D \tag{2}$$

where V_D is the unstressed volume, that is the volume of the vessel at $p_{SV} = 0$. The unstressed volume in the systemic venous circulation is not negligible, as over one-half of the venous volume is unstressed volume [4]; however, we neglect unstressed volume in the other three compliance vessels (see Assumption 2).

The flow q in the vessels of the capillary networks, modeled as in [11] as resistance vessels, is (by Assumption 2):

$$q = \frac{p_A - p_V}{R} \tag{3}$$

Here p_A, p_V and R represent the pressure in the arteries and veins and resistance respectively, in each of the systemic and pulmonary circulation. Thus, there are two equations of the form (3), for systemic and pulmonary capillary flows, distinguished by subscripts S and P respectively on all the variables.

From the Frank-Starling Assumption 4, the following relations for the left and right cardiac outputs, q_L and q_R, respectively, are obtained:

$$q_L = F \cdot C_L \cdot p_{PV} = K_L \cdot p_{PV} \tag{4}$$

$$q_R = F \cdot C_R \cdot p_{SV} = K_R \cdot p_{SV} \tag{5}$$

Here C_L and C_R are the compliances in the left and right hearts respectively and F is the heart beat frequency. The subscripts A and V represent arteries and veins respectively, while S and P stand for the systemic and pulmonary circulations, respectively.

The rate of change of volume of an incompressible fluid in a vessel is the difference between the flow into and the flow out of the vessel. Hence, the following differential equations are obtained, for the change of volume of blood in the systemic arteries, systemic veins, pulmonary arteries and pulmonary veins respectively:

$$\frac{dv_{SA}}{dt} = q_L - q_S \tag{6}$$

$$\frac{dv_{SV}}{dt} = q_S - q_R \tag{7}$$

$$\frac{dv_{PA}}{dt} = q_R - q_P \tag{8}$$

$$\frac{dv_{PV}}{dt} = q_P - q_L \tag{9}$$

q_L, q_R, q_S and q_P, represent blood flow through the left heart, the right heart, the systemic capillaries and the pulmonary capillaries, respectively. At this stage we have twelve equations in twelve unknowns: eight algebraic equations (1)–(5) and four differential equations (6)–(9), in the four volume variables v, four flow variables q and four pressure variables p. The eight algebraic equations may be used to eliminate all eight flow and pressure variables. The result is a system of four differential equations in the four volume variables.

From Assumption 1 that blood is conserved, the following is obtained

$$v_{SA} + v_{SV} + v_{PA} + v_{PV} = V_0 \tag{10}$$

where V_0 is the total blood volume, a constant. Equation (10) indicates that the four volume variables are not independent. As v_{PA} is the smallest, it is chosen for elimination. Then a system of three differential equations in v_{SA}, v_{SV} and v_{PV} is obtained. (Mathematically, any one of the four volume variables could be eliminated.) The resulting mathematical model of the cardiovascular system consists of the following system of three ordinary differential equations:

$$\frac{dv_{SA}}{dt} = -\frac{v_{SA}}{R_S \cdot C_{SA}} + \frac{v_{SV}}{R_S \cdot C_{SV}} + \frac{F \cdot C_L \cdot v_{PV}}{C_{PV}} - \frac{V_D}{R_S \cdot C_{SV}} \tag{11}$$

$$\frac{dv_{SV}}{dt} = \frac{v_{SA}}{R_S \cdot C_{SA}} - \left(\frac{1}{R_S \cdot C_{SV}} + \frac{F \cdot C_R}{C_{SV}}\right)\left(v_{SV} - V_D\right) \tag{12}$$

$$\frac{dv_{PV}}{dt} = \frac{V_0 - v_{SA} - v_{SV} - v_{PV}}{R_P \cdot C_{PA}} - \left(\frac{1}{R_P \cdot C_{PV}} + \frac{F \cdot C_L}{C_{PV}}\right)v_{PV} \tag{13}$$

Note that this model is linear in the three volume variables, represented by lower case v's. The system becomes nonlinear on inclusion of the baroreflex feedback control loops.

2.2.2 Nonlinear baroreflex control

The Hill function is defined by:

$$y = f_n(x) = \frac{x^n}{a^n + x^n}$$
$$f_n(x) : [0, \infty) \to [0, 1) \tag{14}$$

where a is a constant which corresponds to the point of half the maximum output, $f_n(a) = 1/2$. The graph of the Hill function resembles a stretched-out "S". As n increases the graph approaches a perfect step

function or "switch" at $x = a$. The baroreceptor response curve described in the literature strongly resembles a Hill function, and therefore is modeled in this paper as:

$$B_n(p_{SA}) = \frac{(p_{SA})^n}{(P_C)^n + (p_{SA})^n} \tag{15}$$

where B_n is the total baroreceptor afferent activity, n is a measure of the baroreflex gain, and P_C is the critical arterial pressure. The term "gain" normally is used to represent a ratio of the change in output to a change in input, for very small changes. This is essentially the mathematical definition of a derivative. Thus, for our model, using the Hill function for the baroreflex response, we define baroreceptor gain by the derivative

$$\mu = \frac{dB_n}{dp_{SA}} \tag{16}$$

that is, gain μ is equal to the slope of the response function (for fixed n), at a particular point. For simplicity we choose the value of μ at the point $x = a$, which is precisely

$$\mu = \frac{n}{4a}. \tag{17}$$

This is a useful measure of the gain as it is close to the maximum value of the slope (from calculus). Note that we can scale variables so that $a = 1$, and then $\mu = n/4$. Also, note that p_{SA} is proportional to v_{SA} since C_{SA} is a constant, see (1), so B_n can be expressed in terms of v_{SA} rather than p_{SA}. This yields:

$$B_n(p_{SA}) = B_n\left(\frac{v_{SA}}{C_{SA}}\right) = \frac{(v_{SA})^n}{(V_C)^n + (v_{SA})^n} \tag{18}$$

where V_C is the volume at the critical pressure. It should be noted that other functions with a similar graph shape could be used for the baroreceptor response function, for example the hyperbolic tangent function.

Changes in heart rate (F) and systemic capillary resistance (R_S) must be in the opposite direction to a change in arterial blood pressure, in order to restore normal pressure. Thus a simple model of the baroreflex action on F is:

$$F = F_0(1 - B_n) = \frac{F_0(V_C)^n}{(V_C)^n + (v_{SA})^n} \tag{19}$$

where F_0 is a constant. Equation (19) implies that if B approaches 1 (i.e. very large pressure p_{SA}), then F will be zero. However, one would

expect that in reality F will have a non zero minimum value even when B approaches 1. The following is a more realistic representation:

$$F = F_1(1 - B_n) + F_2 = \frac{F_1(V_C)^n}{(V_C)^n + (v_{SA})^n} + F_2 \tag{20}$$

where F_1 and F_2 are constants, and F_2 is the value of F when $B_n = 1$. Similarly, the baroreflex action on systemic resistance R_S is modeled as:

$$R_S = R_1(1 - B_n) + R_2 = \frac{R_1(V_C)^n}{(V_C)^n + (v_{SA})^n} + R_2 \tag{21}$$

On the other hand, changes in systemic venous compliance, C_{SV}, and systemic venous unstressed volume, V_D, act in the same direction as a change in arterial blood pressure. Thus the action of the baroreflex on each of V_D and C_{SV} is modeled as:

$$V_D = D_1 \cdot B_n + D_2 = \frac{D_1(v_{SA})^n}{(V_C)^n + (v_{SA})^n} + D_2 \tag{22}$$

$$C_{SV} = C_1 \cdot B_n + C_2 = \frac{C_1(v_{SA})^n}{(V_C)^n + (v_{SA})^n} + C_2 \tag{23}$$

Now, from the basic linear cardiovascular model (11)–(13), four different nonlinear cardiovascular models are obtained, corresponding to insertion of the baroreceptor feedback function into each of F, R_S, C_{SV} and V_D, as above. This allows independent investigations of each of the four feedback loops, which would be difficult and dangerous to carry out experimentally on live subjects.

2.3 Parameter determination

Many of the parameters in this model are available in the literature, as displayed in Table 1. The remaining parameters, F_1, F_2, R_1, R_2, C_1, C_2, D_1, D_2, C_{SV}, V_C and V_D are not found in the literature and need to be determined.

2.3.1 Critical volume, V_C

No value of V_C was found in the literature. However the normal resting value of v_{SA} is known to be 1.0 litre. It is assumed that the resting and critical states are very close, and hence V_C is taken as 1.0 litre. Since V_C plays the role of a in equation (17) this has the bonus effect of simplifying the formula (17) for the gain, to $\mu = n/4$.

Table 1. Typical parameter values for an adult human being (Hoppensteadt and Peskin [11])

Parameter	Normal value
Compliance in systemic arteries, C_{SA}	0.01 litres/mm Hg
Compliance in pulmonary arteries, C_{PA}	0.00667 litres/mm Hg
Compliance in pulmonary veins, C_{PV}	0.08 litres/mm Hg
Systemic resistance, R_S	17.5 mm Hg/(litre/min.)
Pulmonary resistance, R_P	1.79 mm Hg/(litre/min.)
Compliance in right heart, C_R	0.035 litres/mm Hg
Compliance in left heart, C_L	0.014 litres/mm Hg
Heart rate, F	80 beats/min

2.3.2 Systemic unstressed venous volume, V_D

An exact normal value of V_D is not found in the literature. However, Coleman (1985), gives the value of V_D as "over half" the systemic venous volume v_{SV}. As the normal value of v_{SV} is 3.5 litres, the normal value of V_D is taken to be 2.0 litres in this study.

2.3.3 Systemic venous compliance, C_{SV}

The normal systemic venous compliance is given as 1.75 litres/mm Hg (Hoppensteadt and Peskin, 1992). This value of C_{SV} does not allow for systemic unstressed venous volume, which this study considers. Using Eq. (2), with $v_{SV} = 3.5$ litres, $V_D = 2.0$ litres and $p_{SV} = 2$ mm Hg, the corresponding value of C_{SV} is computed to be 0.75 litres/mm Hg.

2.3.4 Normalized Hill function constants, $F_1, F_2, R_1, R_2, C_1, C_2, D_1$, and D_2

These constants are required for the use of the Hill function to model the baroreceptor afferent activity, B_n, acting on the systemic venous compliance, systemic venous unstretched volume, systemic resistance and heart rate. This current study appears to be the first time such an approach has been taken, which is why these constants are not available. Therefore, different values of each of these constants are investigated in this study, over ranges which yield baroreceptor responses consistent with physiological observations.

3 Analysis and results

The control of the baroreflex on heart rate F, systemic capillary resistance R_S, systemic venous unstressed volume V_D and systemic

venous compliance C_{SV} are investigated individually in the mathematical model. Specifically, the appropriate non-linear baroreflex response function, from (20) to (23), is substituted in each parameter in turn to obtain the corresponding model, which is then investigated for the effects on cardiovascular dynamics. See the Appendixes and [1] for more details. We analyzed each of the four models to find out if a bifurcation occurs as the baroreceptor gain μ varies, using Hopf's bifurcation theorem. First, the steady state solution of each model was calculated. Then the system of equations was linearised at this steady state. Thus the Jacobian matrix (derivative) at the steady state was found. Since it is a real 3×3 matrix, with constant real entries, the eigenvalues are either all three real or else one real and two complex conjugate. The three eigenvalues of the Jacobian matrix were computed symbolically (exactly). In each case there existed, for some values of the gain μ, one real and two complex eigenvalues. The real eigenvalues were always found to be negative. The real part of the pair of complex conjugate eigenvalues was plotted as a function of μ (or n) to find out if a crossing point existed. The symbolic computation of all eigenvalues and the plotting of the curves was done using Maple. A value of μ at which the real part of a complex eigenvalue crosses through zero is known as a Hopf bifurcation point. At this point there exists a pair of purely imaginary eigenvalues $\pm i\omega$ and the steady state is said to be nonhyperbolic. When a crossing point was found, the imaginary part ω of the complex eigenvalues was plotted to obtain its value at the crossing point. Since the third (real) eigenvalue always remained negative, according to the general theory of Liapunov stability, when the real part of the complex eigenvalues crosses from negative to positive the equilibrium state changes from asymptotically stable to unstable. From the Hopf bifurcation theorem [8, 10], generically at such a crossing point, a periodic solution is either created or destroyed. Standard numerical integrations may verify the existence of a stable limit cycle near the crossing point. The imaginary part ω at the crossing point gives a good approximation to the frequency of the resulting oscillations.

3.1 Baroreflex control of heart rate

Models with R_S, C_{SV} and V_D taken as constants and F given by Eq. (20) were considered. Assuming a normal heart rate of 80 beats/min., values of F_1 and F_2 considered were: $F_1 = 160$ beats/min. and $F_2 = 0$ beats/min., $F_1 = 80$ beats/min. and $F_2 = 40$ beats/min., and $F_1 = 40$ beats/min. and $F_2 = 60$ beats/min. All of these models exhibited a stable

steady-state, for all values of gain μ tested. No evidence of waves was found. Details of these models are given in [1].

3.2 Baroreflex control of systemic resistance

Models with the baroreflex affecting only systemic resistance R_S, while C_{SV}, V_D and F are taken as constants, are considered next. R_S is given

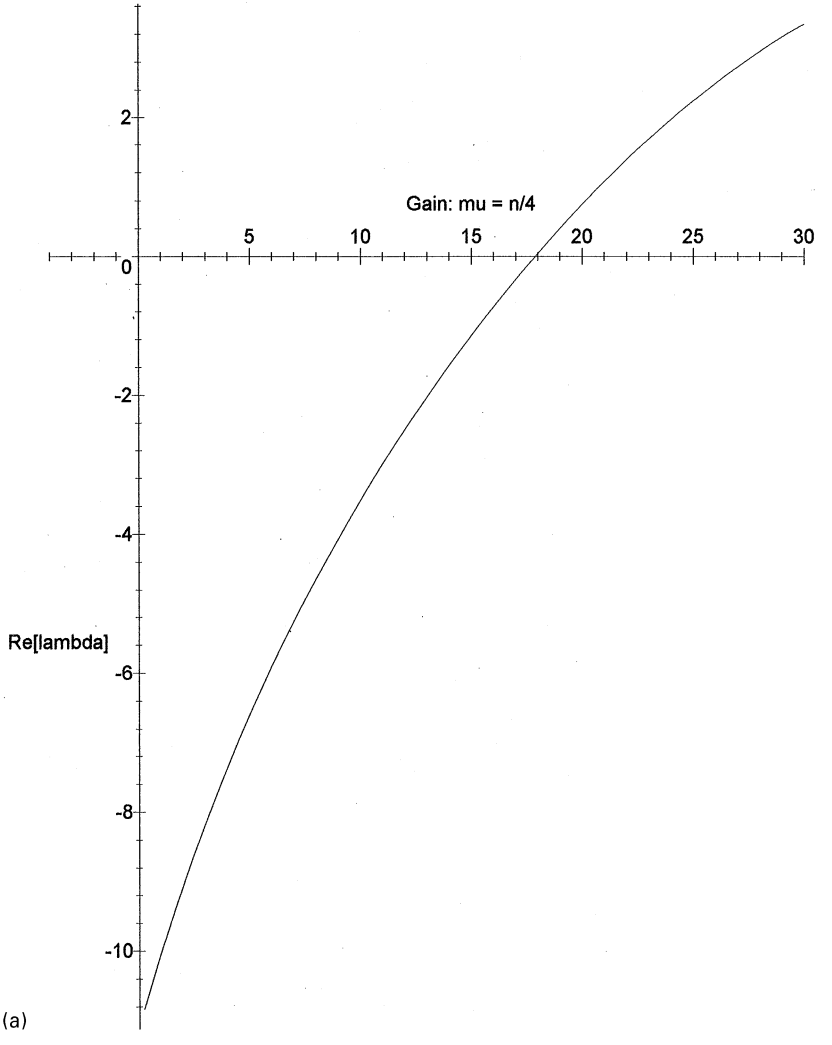

Fig. 1a–d. Re(λ) as a function of gain μ for controlled V_D with **a** $D_2 = 0$ litres; **b** $D_2 = 0.5$ litres; **c** $D_2 = 1.0$ litre; **d** $D_2 = 1.5$ litres

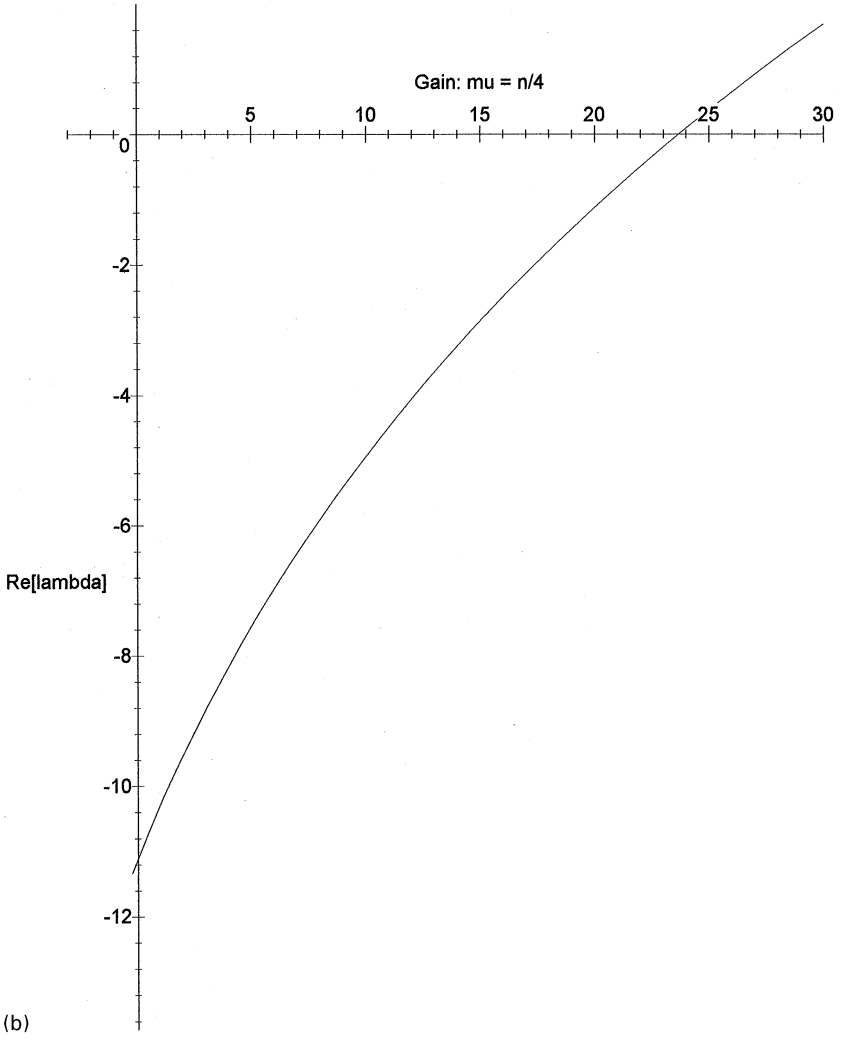

Fig. 1. (continued)

by Eq. (21) and a typical value of systemic resistance is 17.5 mm Hg/(litre/min). Values of R_1 and R_2 used are: $R_1 = 35$ mm Hg/(litre/min) and $R_2 = 0$ mm Hg/(litre/min), $R_1 = 20$ mm Hg/(litre/min) and $R_2 = 7.5$ mm Hg/(litre/min), and $R_1 = 15$ mm Hg/(litre/min) and $R_2 = 10$ mm Hg/(litre/min). These models had a stable steady-state for all values of the gain μ tested, and showed no indications of waves. Details of these models are given in [1].

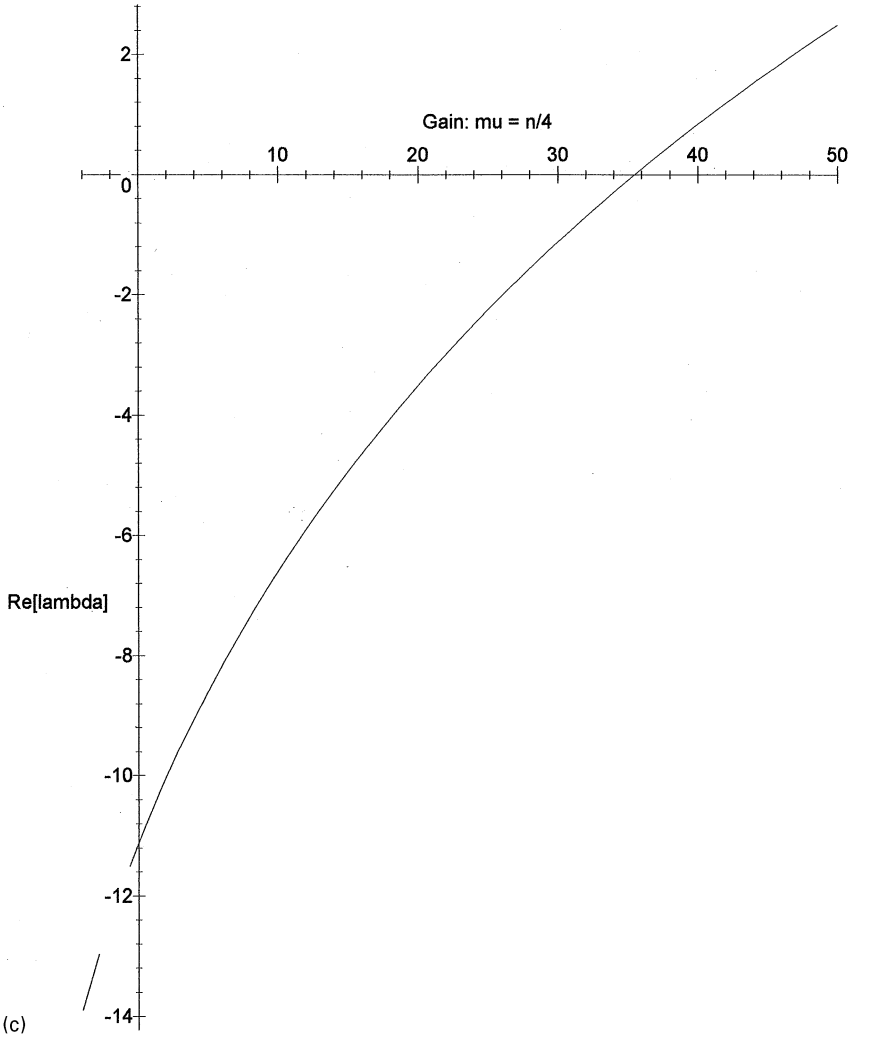

Fig. 1. (continued)

3.3 Baroreflex control of venous volume

The baroreflex may influence the systemic venous volume through both the unstressed or "dead" volume, V_D and the compliance, C_{SV}. Models with the baroreflex controlling C_{SV} and V_D separately were considered (see the Appendix for equations). In both cases the models exhibited unstable steady-states for gains beyond a crossing point with pure imaginary eigenvalues. Figure 1 displays four graphs obtained for models in which the baroreflex controls unstressed venous volume. It

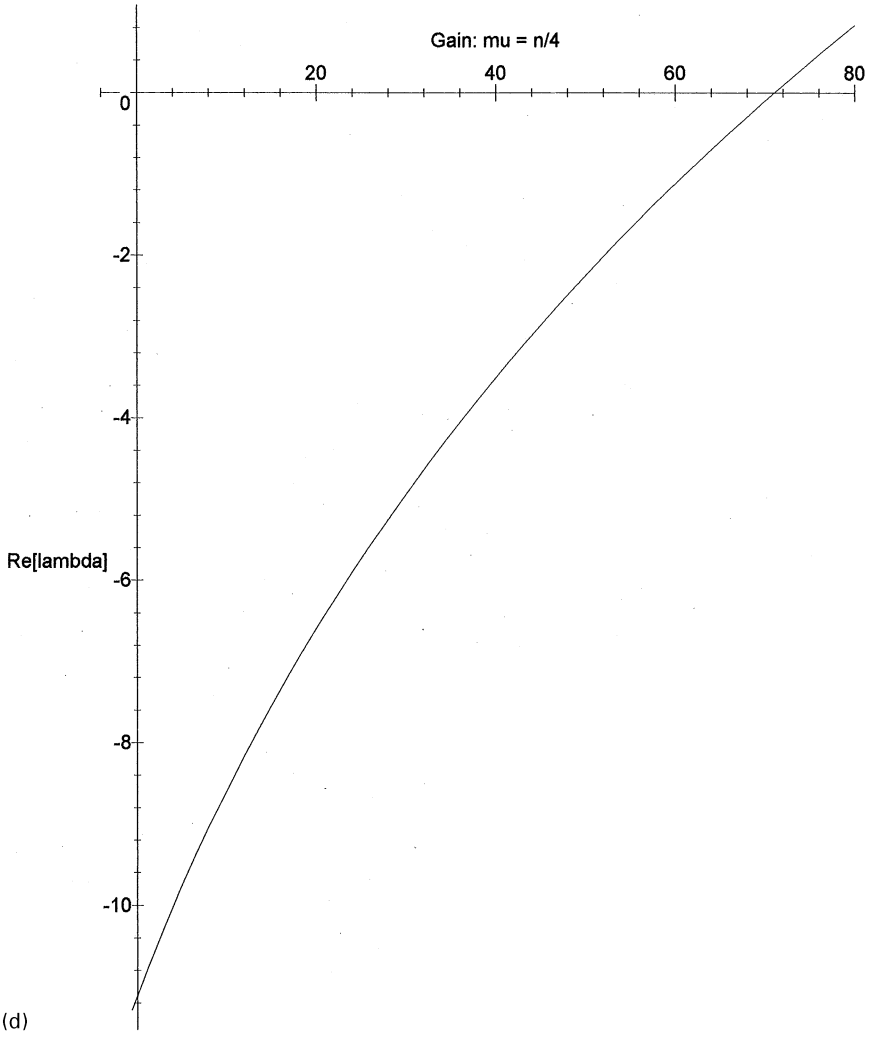

Fig. 1. (continued)

shows graphs of the real parts of the complex eigenvalues, for models with D_2 equal to 0, 0.5, 1.0, and 1.5 litres, respectively. Note that $\mathrm{Re}(\lambda)$ crosses through zero in all cases. This implies a Hopf bifurcation, giving birth to an oscillation (or wave).

Similarly, Fig. 2 is obtained from models with the baroreflex controlling venous compliance only. It shows graphs of the real part of the complex eigenvalues for three cases of models, with C_2 equal to 0, 0.25, and 0.5 litres/mm Hg, respectively. All three cases give a Hopf bifurcation.

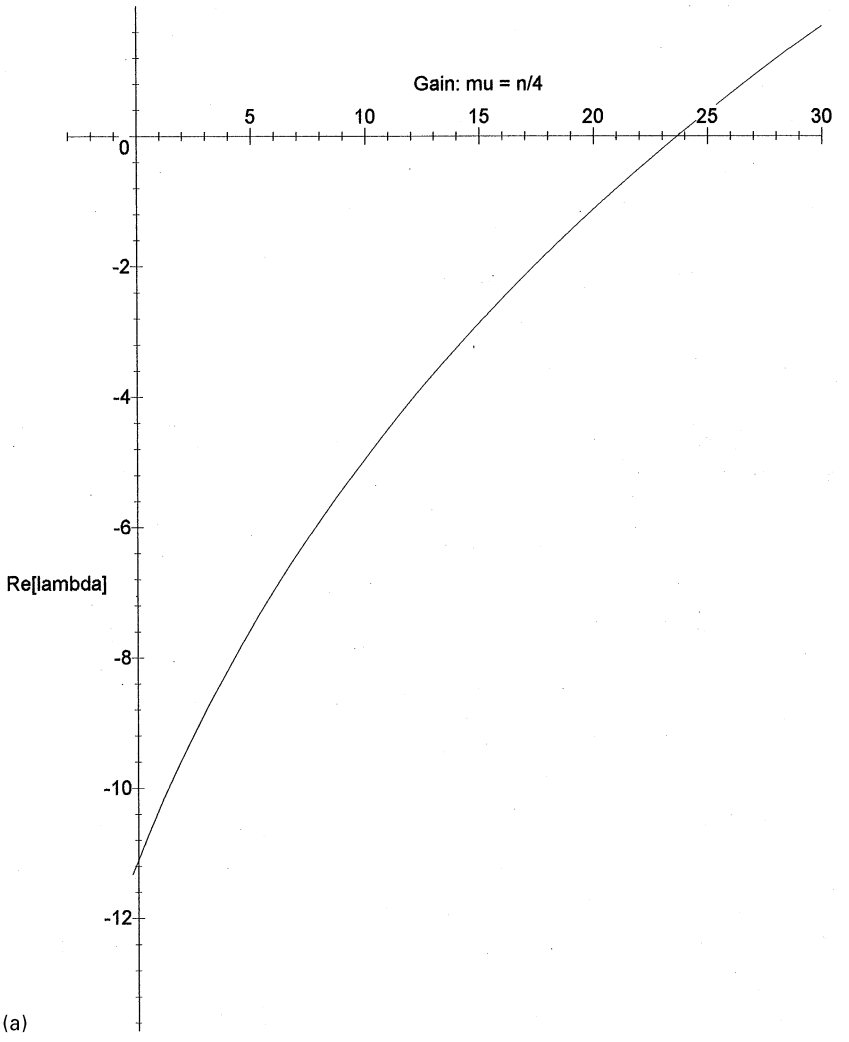

Fig. 2a–c. Re(λ) as a function of gain μ for controlled C_{SV} with **a** $C_2 = 0$ litres/mm Hg; **b** $C_2 = 0.25$ litres/mm Hg; **c** $C_2 = 0.5$ litres/mm Hg

The values of the imaginary parts of the complex eigenvalues at the crossing points give the angular frequency of the oscillations produced. From these frequencies, the periods of oscillation of all these models were found to be between 7 and 12 secs. Note that this is in agreement with reported values of Mayer waves in human subjects.

Figure 3 shows phase portraits obtained by direct numerical integration, for the system with $D_2 = 0$ and gain μ equal to 10 and 20. At $\mu = 10$ ($n = 40$), there exists no limit cycle. However, for $\mu = 20$

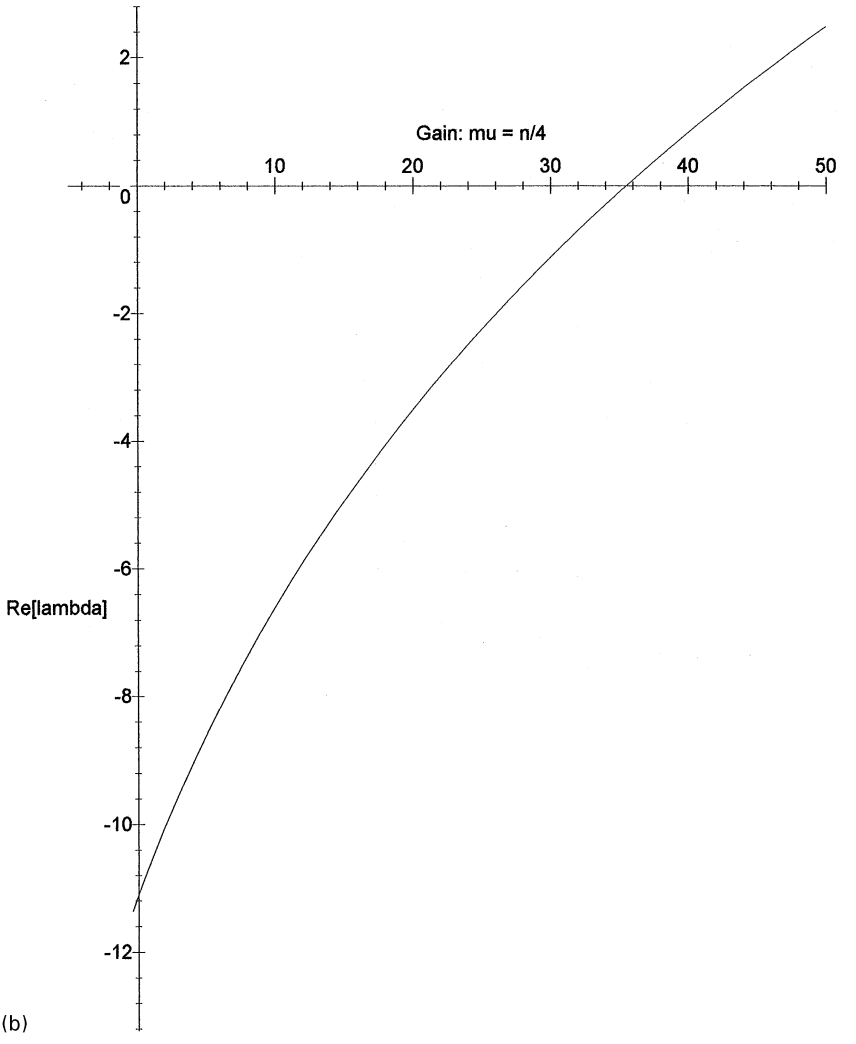

Fig. 2. (continued)

($n = 80$) a limit cycle exists, corroborating our analysis. In the phase portraits of Fig. 3, the three state variables are those of equations (11)–(13), namely

$$\mathrm{A} = v_{SA} = \text{volume of blood in systemic arteries}$$

$$\mathrm{V} = v_{SV} = \text{volume of blood in systemic veins}$$

$$\mathrm{P} = v_{PV} = \text{volume of blood inp ulmonary veins}$$

In all cases considered, when a crossing point existed, a limit cycle was found to be both stable and supercritical (that is, existing for μ greater than the crossing value).

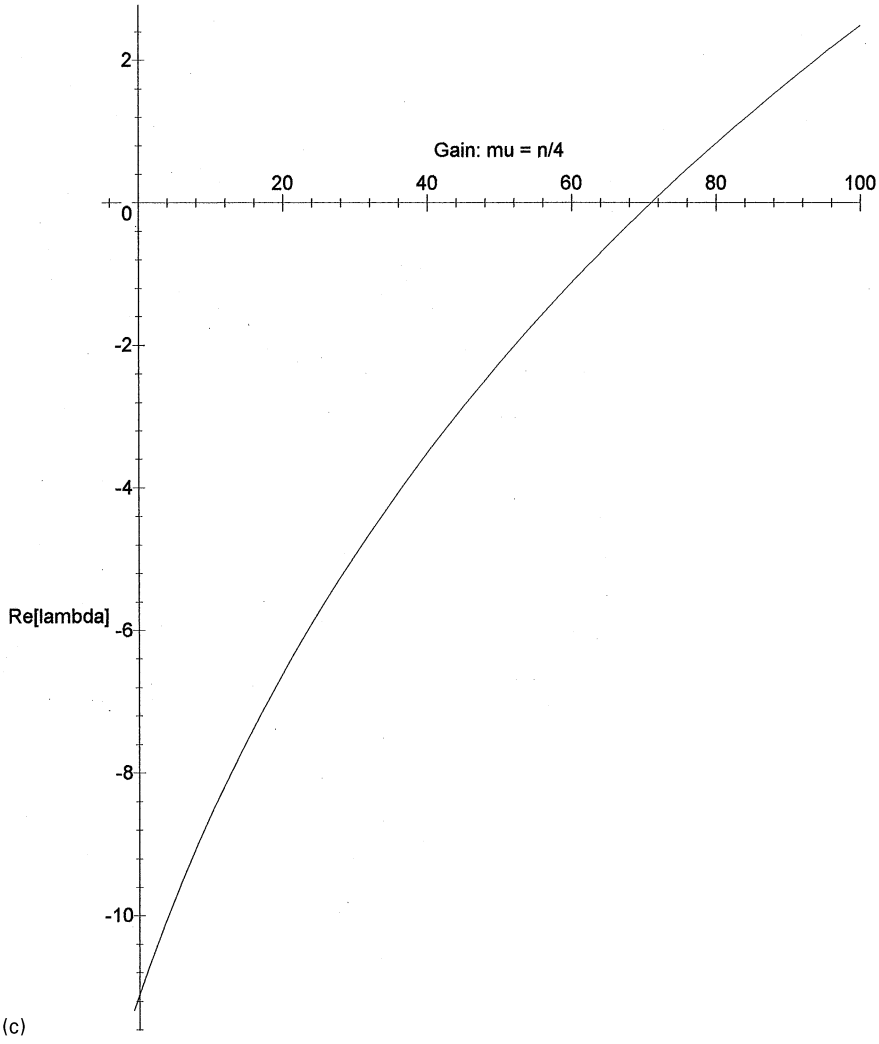

Fig. 2. (continued)

4 Discussion

Models with only heart rate F, or systemic capillary resistance R_S, controlled by the baroreflex did not exhibit a Hopf bifurcation, while the models with systemic venous compliance, C_{SV} or systemic venous unstressed volume, V_D controlled by the baroreflex were capable of Hopf bifurcation. Hence the effect of the baroreflex on F and R_S, individually, is not the cause of oscillations such as Mayer waves. However, if the effect of the baroreflex on F and R_S were combined in

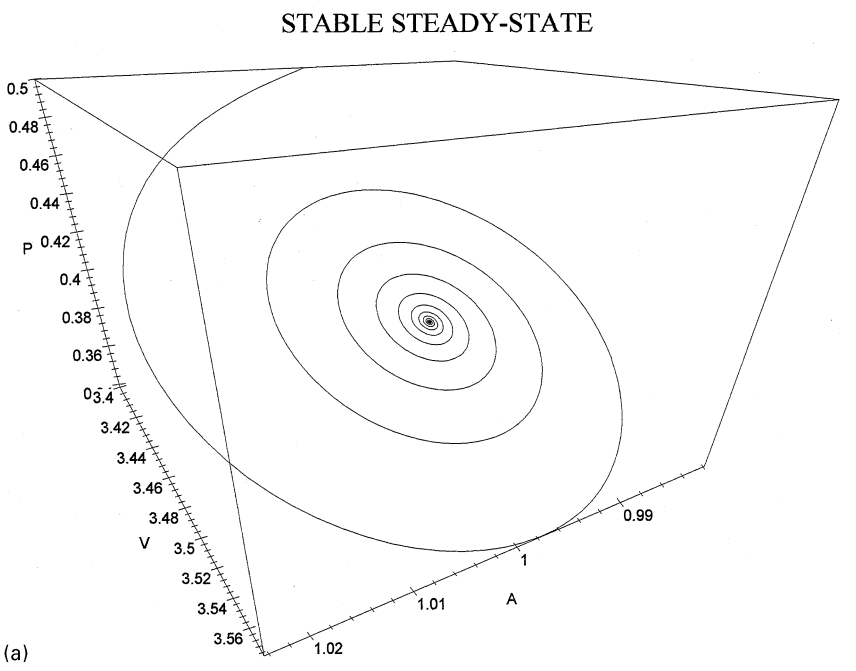

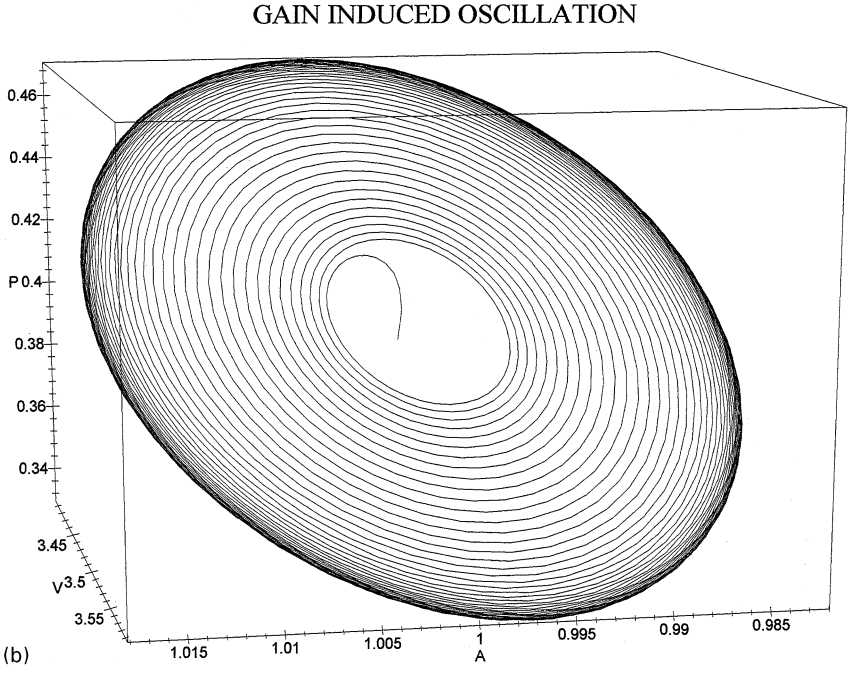

Fig. 3a–c. Phase portraits for controlled V_D with $D_2 = 0$ for **a** $\mu = 10$ and initial point (1.0, 3.4, 0.5); **b** $\mu = 20$ and initial point (1.0, 3.47, 0.39); **c** $\mu = 20$ and initial point (1.0, 3.4, 0.5)

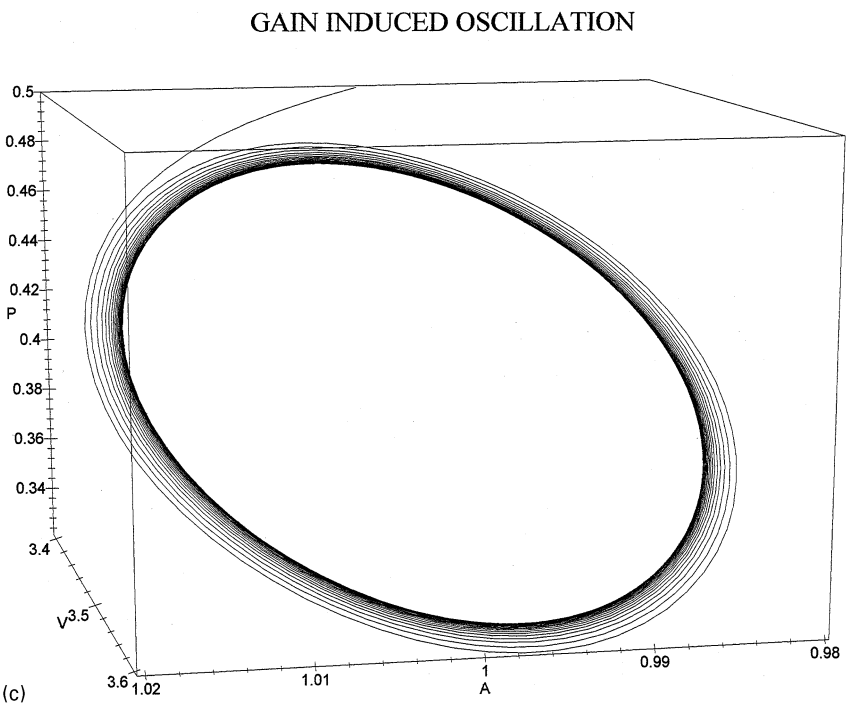

Fig. 3. (continued)

models with the effects on V_D or C_{SV}, they may play a role in the instability.

It is observed that for all models with V_D and C_{SV} individually controlled by the baroreflex, the real part of the complex eigenvalues increases as the gain μ increases and the graph crosses the μ-axis at a positive value of μ. This implies a Hopf bifurcation and the presence of a limit cycle oscillation. The stability of this limit cycle oscillation has been verified numerically. The similarity of the results obtained for models with C_{SV} and V_D individually controlled by the baroreflex is to be expected, as the two have similar effects on blood flow. The model with the baroreflex controlling only C_{SV} is more stable than that with the baroreflex controlling only V_D. This implies a greater sensitivity in the baroreflex control of V_D than of C_{SV}, where gain induced instability is concerned, but control of C_{SV} can not be ignored. Remarkably, the periods of the oscillations fall within the range of 7 to 12 secs. given by Penaz [20].

Measurements by Wesseling et al. [23] on human subjects revealed a periodic fluctuation in heart rate which was synchronized with the Mayer waves in blood pressure. In these experiments, the same period

was observed for the modulation of the heart rate as for the blood pressure waves. The present model provides a satisfactory explanation for this heart rate modulation. Assume that Mayer waves have arisen through the mechanism of this paper, and that all the baroreflex feedback loops are active. Then the baroreceptors would sense a fluctuating blood pressure in the systemic arteries, and would therefore exert a fluctuating feedback control, affecting the heart rate in synchronization with the Mayer waves, as observed in [23].

Further insights were obtained by varying two parameters in the model simultaneously; namely, the gain parameter μ together with either one of D_2 or C_2 (the minimum unstressed systemic venous volume or the compliance, respectively). As either of D_2 or C_2 increases, the value of gain at which the graph crosses the μ-axis increases. This suggests that an increase in D_2 or C_2 increases the stability of the cardiovascular system against oscillations. Changing the value of D_2 or C_2 causes resetting of the baroreceptor curve. This happens in an individual with a time constant of 10 hours and so is not of importance to this investigation. However as different people may have different D_2 and C_2 values, different people can be expected to take different times before Mayer waves are observed, when subjected to identical Mayer wave inducing stresses. In particular it could be expected that young and old people will have different D_2 and C_2 values and this may explain the difference in the incidence in Mayer waves observed in young and old people. As we would expect larger D_2 and C_2 values in older people, corresponding to veins which have become stretched and less fit, our observation that stability increases with increasing values of D_2 and C_2 is in agreement with the age-dependence observed experimentally [6, 11, 13, 16, 18]. In Fig. 4, D_2 is plotted against the crossing point value of gain μ. The top left region represents the parameter values for which the equilibrium state is stable, and corresponds to older subjects, who would tend to have smaller baroreflex gains μ, and larger D_2 values. The lower right region represents unstable equilibria, susceptible to oscillations, and here the parameter values correspond to youths. Thus, stability depends on both the baroreflex gain μ and the venous dead volume D_2. Young adults, with high gain μ and small D_2, are in the unstable region where Mayer waves appear, while older adults with the opposite characteristics are in the stable region where there are no Mayer waves. The same situation holds for μ and C_2.

The principal conclusion of this paper is that the existence of Mayer waves and their disappearance with age may be explained by means of the Hopf bifurcation theorem, as a case of gain induced oscillations.

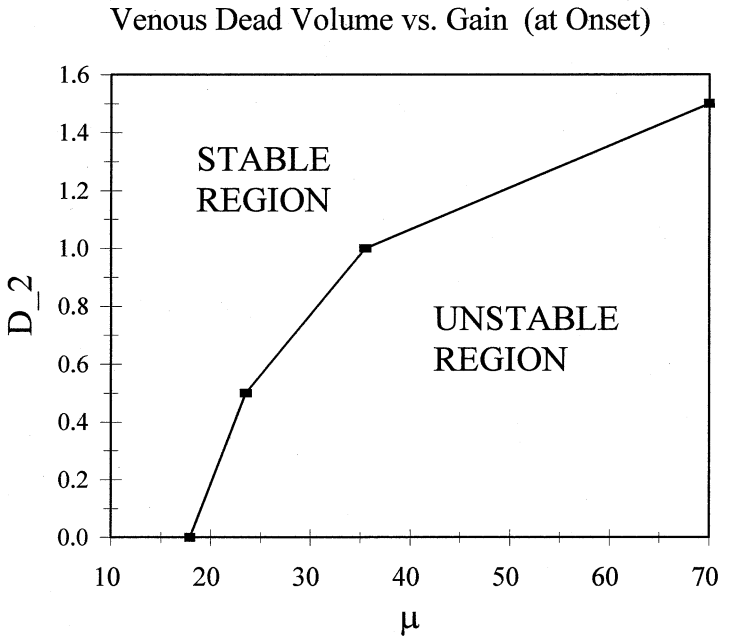

Fig. 4. D_2 as a function of gain μ at the crossing point, for controlled V_D (data points from Fig. 1)

5 Appendix A: Controlled venous volume

The mathematical model has been adapted so that the systemic venous unstressed volume V_D is controlled by the baroreflex, while R_S, C_{SV} and F are assumed to remain constant. The explicit effect on V_D of the baroreflex is given by Eq. (22). Different choices of the constants D_1 and D_2 in (22) were considered. The stability of the equilibrium state was investigated by computation of the eigenvalues of the Jacobian matrix, using Maple, in exact rational arithmetic. The results presented here are expressed in terms of exact rational numbers, free of the roundoff errors which would be introduced by finite decimal representations.

5.1 $D_1 = 4.0$ *litres and* $D_2 = 0$ *litres*

The circulation is then described by the following system of equations:

$$\frac{dv_{SA}}{dt} = -\left(\frac{40}{7}\right)v_{SA} + \left(\frac{8}{105}\right)v_{SV} + 14v_{PV} - \left(\frac{32}{105}\right)\left[\frac{(v_{SA})^{4\mu}}{1+(v_{SA})^{4\mu}}\right]$$

$$\frac{dv_{SV}}{dt} = \frac{40}{7} v_{SA} - \frac{80}{21} v_{SV} + \left(\frac{320}{21}\right)\left[\frac{(v_{SA})^{4\mu}}{1 + (v_{SA})^{4\mu}}\right]$$

$$\frac{dv_{PV}}{dt} = 420 - 84v_{SA} - 84v_{SV} - 105v_{PV}$$

The steady state values of the system are found to be: $v_{SA} = 1.0$ litres, $v_{SV} = 3.5$ litres, and $v_{PV} = 0.4$ litres. Linearization of the model at the steady state gives the matrix A.

$$A = \begin{pmatrix} \dfrac{-40}{7} - \dfrac{32\mu}{105} & \dfrac{8}{105} & 14 \\ \dfrac{40}{7} + \dfrac{320\mu}{21} & -\dfrac{80}{21} & 0 \\ -84 & -84 & -105 \end{pmatrix}$$

The eigenvalues of A are:

$$\lambda_1 = U^{1/3} - V - \frac{2405}{63} - \frac{32\mu}{315}$$

$$\lambda_2 = \frac{U^{1/3}}{2} + \frac{V}{2} - \frac{2405}{63} - \frac{32\mu}{315} + \frac{\mathrm{i}}{2}\sqrt{3}(U^{1/3} + V)$$

$$\lambda_3 = \frac{U^{1/3}}{2} + \frac{V}{2} - \frac{2405}{63} - \frac{32\mu}{315} - \frac{\mathrm{i}}{2}\sqrt{3}(U^{1/3} + V)$$

where

$$U = \frac{-5\,103\,633\,725}{250\,047} - \frac{3\,618\,065\,648\mu}{416\,745} + \frac{184\,832\mu^2}{416\,745} - \frac{32\,768\mu^3}{31\,255\,875}$$

$$+ \frac{8}{2835}(4\,488\,999\,170\,550 + 45\,082\,290\,017\,400\mu$$

$$+ 9\,458\,754\,238\,932\mu^2 - 942\,218\,496\mu^3 + 2\,248\,704\mu^4)^{1/2}$$

and

$$V = U^{-1/3}\left(\frac{-2\,876\,953}{3969} + \frac{11552\mu}{3969} - \frac{1024\mu^2}{99225}\right)$$

For values of μ of interest, eigenvalue λ_1 is real and negative. Eigenvalues λ_2 and λ_3 are complex conjugates, with real part which crosses through zero from negative to positive as μ increases, near $\mu = 18$, as shown in Fig. 1a. Phase portraits, on each side of the crossing point, are shown in Fig. 3.

5.2 $D_1 = 3.0$ litres and $D_2 = 0.5$ litres

The circulation is then described by the following system of equations:

$$\begin{aligned}
\frac{dv_{SA}}{dt} &= -\left(\frac{40}{7}\right)v_{SA} + \left(\frac{8}{105}\right)v_{SV} + 14v_{PV} - \left(\frac{4}{105}\right)\left[\frac{1 + 7(v_{SA})^{4\mu}}{1 + (v_{SA})^{4\mu}}\right] \\
\frac{dv_{SV}}{dt} &= \left(\frac{40}{7}\right)v_{SA} - \left(\frac{80}{21}\right)v_{SV} + \left(\frac{40}{21}\right)\left[\frac{1 + 7(v_{SA})^{4\mu}}{1 + (v_{SA})^{4\mu}}\right] \qquad (24) \\
\frac{dv_{PV}}{dt} &= 420 - 84v_{SA} - 84v_{SV} - 105v_{PV}
\end{aligned}$$

The steady state values of the system are found to be: $v_{SA} = 1.0$ litres, $v_{SV} = 3.5$ litres, and $v_{PV} = 0.4$ litres. Linearization of the model at the steady state gives the matrix A.

$$A = \begin{pmatrix} \dfrac{-40}{7} - \dfrac{8\mu}{35} & \dfrac{8}{105} & 14 \\ \dfrac{40}{7} + \dfrac{80\mu}{7} & -\dfrac{80}{21} & 0 \\ -84 & -84 & -105 \end{pmatrix}$$

The eigenvalues of A are:

$$\lambda_1 = U^{1/3} - V - \frac{2405}{63} - \frac{8\mu}{105}$$

$$\lambda_2 = \frac{U^{1/3}}{2} + \frac{V}{2} - \frac{2405}{63} - \frac{8\mu}{105} + \frac{\mathrm{i}}{2}\sqrt{3}(U^{1/3} + V)$$

$$\lambda_3 = \frac{U^{1/3}}{2} + \frac{V}{2} - \frac{2405}{63} - \frac{8\mu}{105} - \frac{\mathrm{i}}{2}\sqrt{3}(U^{1/3} + V)$$

where

$$\begin{aligned}
U = {} & \frac{-5\,103\,633\,725}{250\,047} - \frac{904\,516\,412\mu}{138\,915} + \frac{11\,552\mu^2}{46\,305} - \frac{512\mu^3}{1\,157\,625} \\
& + \frac{4}{2835}(17\,955\,996\,682\,200 + 135\,246\,870\,052\,200\mu \\
& + 21\,282\,197\,037\,597\mu^2 - 1\,589\,993\,712\mu^3 + 2\,846\,016\mu^4)^{1/2}
\end{aligned}$$

and

$$V = U^{-1/3}\left(\frac{-2\,876\,953}{3969} + \frac{2888\mu}{1323} - \frac{64\mu^2}{11\,025}\right)$$

For values of μ of interest, eigenvalue λ_1 is real and negative. Eigenvalues λ_2 and λ_3 are complex conjugates, with real part which crosses through zero from negative to positive as μ increases, near $\mu = 24$, as shown in Fig. 1b.

5.3 $D_1 = 2.0$ litres and $D_2 = 1.0$ litres

The circulation is then described by the following system of equations:

$$\frac{dv_{SA}}{dt} = -\left(\frac{40}{7}\right)v_{SA} + \left(\frac{8}{105}\right)v_{SV} + 14v_{PV} - \left(\frac{8}{105}\right)\left[\frac{1 + 3(v_{SA})^{4\mu}}{1 + (v_{SA})^{4\mu}}\right]$$

$$\frac{dv_{SV}}{dt} = \left(\frac{40}{7}\right)v_{SA} - \left(\frac{80}{21}\right)v_{SV} + \left(\frac{80}{21}\right)\left[\frac{1 + 3(v_{SA})^{4\mu}}{1 + (v_{SA})^{4\mu}}\right]$$

$$\frac{dv_{PV}}{dt} = 420 - 84v_{SA} - 84v_{SV} - 105v_{PV}$$

The steady state of the system is found at: $v_{SA} = 1.0$ litres, $v_{SV} = 3.5$ litres, and $v_{PV} = 0.4$ litres. Linearization of the model at the steady state gives the matrix A.

$$A = \begin{pmatrix} \frac{-40}{7} & -\frac{16\mu}{105} & \frac{8}{105} & 14 \\ \frac{40}{7} & +\frac{160\mu}{21} & -\frac{80}{21} & 0 \\ & -84 & -84 & -105 \end{pmatrix}$$

The eigenvalues of A are:

$$\lambda_1 = U^{1/3} - V - \frac{2405}{63} - \frac{16\mu}{315}$$

$$\lambda_2 = \frac{U^{1/3}}{2} + \frac{V}{2} - \frac{2405}{63} - \frac{16\mu}{315} + \frac{\mathrm{i}}{2}\sqrt{3}(U^{1/3} + V)$$

$$\lambda_3 = \frac{U^{1/3}}{2} + \frac{V}{2} - \frac{2405}{63} - \frac{16\mu}{315} - \frac{\mathrm{i}}{2}\sqrt{3}(U^{1/3} + V)$$

where

$$U = \frac{-5\,103\,633\,725}{250\,047} - \frac{1\,809\,032\,824\mu}{416\,745} + \frac{46\,208\mu^2}{416\,745} - \frac{4096\mu^3}{31\,255\,875}$$

$$+ \frac{8}{2835}(4\,488\,999\,170\,550 + 22\,541\,145\,008\,700\mu$$

$$+ 2\,364\,688\,559\,733\mu^2 - 117\,777\,312\mu^3 + 140\,544\mu^4)^{1/2}$$

and

$$V = U^{-1/3}\left(\frac{-2\,876\,953}{3969} + \frac{5776\mu}{3969} - \frac{256\mu^2}{99\,225}\right)$$

For values of μ of interest, eigenvalue λ_1 is real and negative. Eigenvalues λ_2 and λ_3 are complex conjugates, with real part which crosses through zero from negative to positive as μ increases, near $\mu = 36$, as shown in Fig. 1c.

5.4 $D_1 = 1.0$ litres and $D_2 = 1.5$ litres

The circulation is then described by the following system of equations:

$$\frac{dv_{SA}}{dt} = -\left(\frac{40}{7}\right)v_{SA} + \left(\frac{8}{105}\right)v_{SV} + 14v_{PV} - \left(\frac{4}{105}\right)\left[\frac{3 + 5(v_{SA})^{4\mu}}{1 + (v_{SA})^{4\mu}}\right]$$

$$\frac{dv_{SV}}{dt} = \left(\frac{40}{7}\right)v_{SA} - \left(\frac{80}{21}\right)v_{SV} + \left(\frac{40}{21}\right)\left[\frac{3 + 5(v_{SA})^{4\mu}}{1 + (v_{SA})^{4\mu}}\right]$$

$$\frac{dv_{PV}}{dt} = 420 - 84v_{SA} - 84v_{SV} - 105v_{PV}$$

The steady state values of the system are found to be: $v_{SA} = 1.0$ litres, $v_{SV} = 3.5$ litres, and $v_{PV} = 0.4$ litres. Linearization of the model at the steady state gives the matrix A.

$$A = \begin{pmatrix} \frac{-40}{7} & -\frac{8\mu}{105} & \frac{8}{105} & 14 \\ \frac{40}{7} + \frac{80\mu}{21} & & -\frac{80}{21} & 0 \\ -84 & & -84 & -105 \end{pmatrix}$$

The eigenvalues of A are:

$$\lambda_1 = U^{1/3} - V - \frac{2405}{63} - \frac{8\mu}{315}$$

$$\lambda_2 = \frac{U^{1/3}}{2} + \frac{V}{2} - \frac{2405}{63} - \frac{8\mu}{315} + \frac{\mathrm{i}}{2}\sqrt{3}(U^{1/3} + V)$$

$$\lambda_3 = \frac{U^{1/3}}{2} + \frac{V}{2} - \frac{2405}{63} - \frac{8\mu}{315} - \frac{\mathrm{i}}{2}\sqrt{3}(U^{1/3} + V)$$

where

$$U = \frac{-5\,103\,633\,725}{250\,047} - \frac{904\,516\,412\mu}{416\,745} + \frac{11\,552\mu^2}{416\,745} - \frac{512\mu^3}{31\,255\,875}$$

$$+ \frac{4}{2835}(17\,955\,996\,682\,200 + 45\,082\,290\,017\,400\mu$$

$$+ 2\,364\,688\,559\,733\mu^2 - 58\,888\,656\mu^3 + 35\,136\mu^4)^{1/2}$$

and

$$V = U^{-1/3}\left(\frac{-2\,876\,953}{3969} + \frac{2888\mu}{3969} - \frac{64\mu^2}{99\,225}\right)$$

For values of μ of interest, eigenvalue λ_1 is real and negative. Eigenvalues λ_2 and λ_3 are complex conjugates, with real part which crosses through zero from negative to positive as μ increases, near $\mu = 71$, as shown in Fig. 1d.

6 Appendix B: Controlled venous compliance

A mathematical model was constructed in which the systemic venous compliance C_{SV} is controlled by the baroreflex, while R_s, V_D and F, are held constant. C_{SV} is given by Eq. (23). The stability of the model, for different values of C_1 and C_2 was explored. The results of these calculations are presented in Fig. 2.

6.1 $C_1 = 1.5$ litres/mm Hg and $C_2 = 0$ litres/mm Hg

The circulation is then described by the following system of equations:

$$\frac{dv_{SA}}{dt} = -\left(\frac{40}{7}\right)v_{SA} + \left(\frac{4}{105}\right)v_{SV}\left[\frac{1 + (v_{SA})^{4\mu}}{(v_{SA})^{4\mu}}\right]$$

$$+ 14v_{PV} - \left(\frac{8}{105}\right)\left[\frac{1 + (v_{SA})^{4\mu}}{(v_{SA})^{4\mu}}\right]$$

$$\frac{dv_{SV}}{dt} = \left(\frac{40}{7}\right)v_{SA} - \left(\frac{40}{21}\right)v_{SV}\left[\frac{1 + (v_{SA})^{4\mu}}{(v_{SA})^{4\mu}}\right] + \left(\frac{80}{21}\right)\left[\frac{1 + (v_{SA})^{4\mu}}{(v_{SA})^{4\mu}}\right]$$

$$\frac{dv_{PV}}{dt} = 420 - 84v_{SA} - 84v_{SV} - 105v_{PV}$$

The steady state of the system is found to be: $v_{SA} = 1.0$ litres, $v_{SV} = 3.5$ litres, and $v_{P_v} = 0.4$ litres. Linearization of the model at the steady state gives the matrix A.

$$A = \begin{pmatrix} \dfrac{-40}{7} & -\dfrac{8\mu}{35} & \dfrac{8}{105} & 14 \\ \dfrac{40}{7} + \dfrac{80\mu}{21} & & -\dfrac{80}{21} & 0 \\ -84 & & -84 & -105 \end{pmatrix}$$

The eigenvalues of A are:

$$\lambda_1 = U^{1/3} - V - \frac{2405}{63} - \frac{8\mu}{105}$$

$$\lambda_2 = \frac{U^{1/3}}{2} + \frac{V}{2} - \frac{2405}{63} - \frac{8\mu}{105} + \frac{\mathrm{i}}{2}\sqrt{3}(U^{1/3} + V)$$

$$\lambda_3 = \frac{U^{1/3}}{2} + \frac{V}{2} - \frac{2405}{63} - \frac{8\mu}{105} - \frac{\mathrm{i}}{2}\sqrt{3}(U^{1/3} + V)$$

where

$$U = \frac{-5\,103\,633\,725}{250\,047} - \frac{904\,516\,412\mu}{138\,915} + \frac{11\,552\mu^2}{46\,305} - \frac{512\mu^3}{1\,157\,625}$$

$$+ \frac{4}{2835}(17\,955\,996\,682\,200 + 135\,246\,870\,052\,200\mu$$

$$+ 21\,282\,197\,037\,597\mu^2 - 1\,589\,993\,712\mu^3 + 2\,846\,016\mu^4)^{1/2}$$

and

$$V = U^{-1/3}\left(\frac{-2\,876\,953}{3969} + \frac{2888\mu}{1323} - \frac{64\mu^2}{11\,025}\right)$$

For values of μ of interest, eigenvalue λ_1 is real and negative. Eigenvalues λ_2 and λ_3 are complex conjugates, with real part which crosses through zero from negative to positive as μ increases, near $\mu = 24$, as shown in Fig. 2a.

6.2 $C_1 = 1.0$ l/mm Hg and $C_2 = 0.25$ l/mm Hg

The circulation is then described by the following system of equations:

$$\frac{dv_{SA}}{dt} = -\left(\frac{40}{7}\right)v_{SA} + \left(\frac{8}{35}\right)v_{SV}\left[\frac{1 + (v_{SA})^{4\mu}}{1 + 5(v_{SA})^{4\mu}}\right] + 14v_{PV} - \left(\frac{16}{35}\right)\left[\frac{1 + (v_{SA})^{4\mu}}{1 + 5(v_{SA})^{4\mu}}\right]$$

$$\frac{dv_{SV}}{dt} = \left(\frac{40}{7}\right)v_{SA} - \left(\frac{80}{7}\right)v_{SV}\left[\frac{1 + (v_{SA})^{4\mu}}{1 + 5(v_{SA})^{4\mu}}\right] + \left(\frac{160}{7}\right)\left[\frac{1 + (v_{SA})^{4\mu}}{1 + 5(v_{SA})^{4\mu}}\right]$$

$$\frac{dv_{PV}}{dt} = 420 - 84v_{SA} - 84v_{SV} - 105v_{PV}$$

The steady state values of the system are found to be: $v_{SA} = 1.0$ litres, $v_{SV} = 3.5$ litres, and $v_{PV} = 0.4$ litres. Linearization of the model at the steady state gives the matrix A.

$$A = \begin{pmatrix} \dfrac{-40}{7} - \dfrac{16\mu}{105} & \dfrac{8}{105} & 14 \\ \dfrac{40}{7} + \dfrac{160\mu}{21} & -\dfrac{80}{21} & 0 \\ -84 & -84 & -105 \end{pmatrix}$$

The eigenvalues of A are:

$$\lambda_1 = U^{1/3} - V - \frac{2405}{63} - \frac{16\mu}{315}$$

$$\lambda_2 = \frac{U^{1/3}}{2} + \frac{V}{2} - \frac{2405}{63} - \frac{16\mu}{315} + \frac{\mathrm{i}}{2}\sqrt{3}(U^{1/3} + V)$$

$$\lambda_3 = \frac{U^{1/3}}{2} + \frac{V}{2} - \frac{2405}{63} - \frac{16\mu}{315} - \frac{\mathrm{i}}{2}\sqrt{3}(U^{1/3} + V)$$

where

$$U = \frac{-5\,103\,633\,725}{250\,047} - \frac{1\,809\,032\,824\mu}{416\,745} + \frac{46208\mu^2}{416\,745} - \frac{4096\mu^3}{31\,255\,875} + \frac{8}{2835}(4\,488\,999\,170\,550 + 22\,541\,145\,008\,700\mu + 2\,364\,688\,559\,733\mu^2 - 117\,777\,312\mu^3 + 140\,544\mu^4)^{1/2}$$

and

$$V = U^{-1/3}\left(\frac{-2\,876\,953}{3969} + \frac{5776\mu}{3969} - \frac{256\mu^2}{99\,225}\right)$$

For values of μ of interest, eigenvalue λ_1 is real and negative. Eigenvalues λ_2 and λ_3 are complex conjugates, with real part which crosses through zero from negative to positive as μ increases, near $\mu = 36$, as shown in Fig. 2b.

6.3 $C_1 = 0.5$ l/mm Hg and $C_2 = 0.5$ l/mm Hg

The cardiovascular circulation is then described by the following system of equations:

$$\frac{dv_{SA}}{dt} = -\left(\frac{40}{7}\right)v_{SA} + \left(\frac{4}{35}\right)v_{SV}\left[\frac{1 + (v_{SA})^{4\mu}}{1 + 2(v_{SA})^{4\mu}}\right] + 14v_{PV} - \left(\frac{8}{35}\right)\left[\frac{1 + (v_{SA})^{4\mu}}{1 + 2(v_{SA})^{4\mu}}\right]$$

$$\frac{dv_{SV}}{dt} = \left(\frac{40}{7}\right)v_{SA} - \left(\frac{40}{7}\right)v_{SV}\left[\frac{1 + (v_{SA})^{4\mu}}{1 + 2(v_{SA})^{4\mu}}\right] + \left(\frac{80}{7}\right)\left[\frac{1 + (v_{SA})^{4\mu}}{1 + 2(v_{SA})^{4\mu}}\right]$$

$$\frac{dv_{PV}}{dt} = 420 - 84v_{SA} - 84v_{SV} - 105v_{PV}$$

The steady state of the system was found to be: $v_{SA} = 1.0$ litres, $v_{SV} = 3.5$ litres, and $v_{PV} = 0.4$ litres. Linearization of the model at the steady state gives the matrix A.

$$A = \begin{pmatrix} \dfrac{-40}{7} - \dfrac{8\mu}{105} & \dfrac{8}{105} & 14 \\ \dfrac{40}{7} + \dfrac{80\mu}{21} & -\dfrac{80}{21} & 0 \\ -84 & -84 & -105 \end{pmatrix}$$

The eigenvalues of A are:

$$\lambda_1 = U^{1/3} - V - \frac{2405}{63} - \frac{8\mu}{315}$$

$$\lambda_2 = \frac{U^{1/3}}{2} + \frac{V}{2} - \frac{2405}{63} - \frac{8\mu}{315} + \frac{\mathrm{i}}{2}\sqrt{3}(U^{1/3} + V)$$

$$\lambda_3 = \frac{U^{1/3}}{2} + \frac{V}{2} - \frac{2405}{63} - \frac{8\mu}{315} - \frac{\mathrm{i}}{2}\sqrt{3}(U^{1/3} + V)$$

where

$$U = \frac{-5\,103\,633\,725}{250\,047} - \frac{904\,516\,412\mu}{416\,745} + \frac{11\,552\mu^2}{416\,745} - \frac{512\mu^3}{31\,255\,875}$$

$$+ \frac{4}{2835}(17\,955\,996\,682\,200 + 45\,082\,290\,017\,400\mu$$

$$+ 2\,364\,688\,559\,733\mu^2 - 58\,888\,656\mu^3 + 35136\mu^4)^{1/2}$$

and

$$V = U^{-1/3}\left(\frac{-2\,876\,953}{3969} + \frac{2888\mu}{3969} - \frac{64\mu^2}{99\,225}\right)$$

For values of μ of interest, eigenvalue λ_1 is real and negative. Eigenvalues λ_2 and λ_3 are complex conjugates, with real part which crosses through zero from negative to positive as μ increases, near $\mu = 71$, as shown in Fig. 2c.

References

1. Abbiw-Jackson, R. M.: Gain Induced Instability in Blood Pressure (M.Sc. Thesis). Univ. of Guelph, Canada, 1997
2. Anderson, B. A., Kenney, R. A., Neil, E.: The role of the chemoceptors of the carotid and aortic regions in the production of the Mayer waves. Acta. physiol. scand. **20** (1950) 203–220
3. Avula, X. A. J., Ostreicher, H. L.: Mathematical model of the cardiovascular system under acceleration stress. Aviat. Space Environ. Med. **49** (1978) 279–286
4. Coleman, T. G.: Mathematical analysis of cardiovascular function. IEEE Trans. Biomed. Eng. **32** (1985) 289–294
5. Deboer, R. W., Karemaker, J. M., Strackee, J.: Hemodynamic fluctuations and baroreflex sensitivity in humans: a beat to beat model. Am. J. Physiol. **253** (1987) 680–689
6. Epstein, S. E., Stampfer, M., Beiser, G. D.: Role of the capacitance and resistance vessels in vasovagal syncope. Circulation. **37** (1968) 524–533
7. Glass, L., Mackey, M. C.: From Clocks to Chaos: The Rhythms of Life. New Jersey: Princeton University Press, 1988
8. Golubitsky, M., Langford, W. F.: Classification and unfoldings of degenerate Hopf bifurcations. J. Diff. Eq. **41** (1981) 375–415
9. Hale, J.: Theory of Functional Differential Equations. New York: Springer-Verlag, 1977
10. Hassard, B. D., Kazarinoff, N. D., Wan, Y. H.: Theory and Applications of Hopf Bifurcation. Cambridge: Cambridge University Press, 1981
11. Hoppensteadt, F. C., Peskin, C. S.: Mathematics in Medicine and the Life Sciences. New York: Springer-Verlag, 1992
12. Jarisch, W. R., Ferguson, J. J., Shannon, R. P., Wei, J. Y., Goldberger, A. L.: Experientia. **43** (1987) 1207–1209

13. Kanoh, H.: Analysis by a mathematical model. In: Miyakawa, K., Koepchen, H. P., Polosa. C. (eds) Mechanisms of Blood Pressure Waves. Berlin: Springer-Verlag, 1984, pp. 241–254
14. Kaplan, D. T., Furman, M. I., Pincus, S. M., Ryan, S. M., Lipsitz, L. A., Goldberger, A. L.: Aging and the complexity of cardiovascular dynamics. Biophys. J. **59** (1991) 945–949
15. Langford, W. F.: Numerical solution of bifurcation problems for ordinary differential equations. Numer. Math. **28** (1977) 171–190
16. Lipsitz, L. A., Goldberger, A. L.: Loss of complexity and aging: Potential applications of fractals and chaos theory to senescence. JAMA **267** (1992) 1806–1809
17. Mayer, S.: Studien zur Physiologie des Herzens und der Blutgefasse: 5. Abhandlung: Uber spontane Blutdruckschwankungen. Sber. Akad. Wiss. Wien. **74** (1876) 281–307
18. McLeod, J.: PHYSBE – A physiological simulation benchmark experiment. Simulation. **7** (1996) 324–329
19. Miyamoto, Y., Higuchi, J., Mikami, T.: Cardiorespiratory dynamics during vasovagal syncope induced by a head-up tilt. Japan J. Physiol. **32** (1982) 885–889
20. Penaz, J.: Mayer Waves: History and methodology. Automedica. **2** (1978) 135–141
21. Pontryagin, L. S.: Ordinary Differential Equations. Addison-Wesley, 1962
22. Shoukas, A. A., Sagawa, K.: Control of total systemic vascular capacity by the carotid sinus baroreceptor reflex. Cir. Res. **33** (1973) 22–33
23. Wesseling, K. H., Settels, J. J., Walstra, G., Van Esch, H. J., Donders, J. H.: Baromodulation as the cause of short term blood pressure variability? In: Alberni, G., Bajzer, Z., Baxa, P. (eds) Proceedings of the International Conference on Application of Physics to Medicine and Biology, Trieste, 1982, Singapore: World Scientific, 1983, pp. 247–276
24. Wesseling, K. H., Settels, J. J.: Baromodulation explains short-term blood pressure variability. In: Orlebeke, J. F., Mulder, G., Van Doorman, L. J. P. (eds) Psychophysiology of Cardiovascular Control, New York: Plenum Press, 1985, pp. 69–97